prosthesis

MDPI

Article

Flexural Properties of Three Novel 3D-Printed Dental Resins Compared to Other Resin-Based Restorative Materials

Francesco De Angelis [1,*,†], Maurizio D'Amario [2,†], Ali Jahjah [2], Massimo Frascaria [2], Mirco Vadini [1], Edoardo Sorrentino [1], Virginia Biferi [1,‡] and Camillo D'Arcangelo [1,‡]

[1] Unit of Restorative Dentistry and Endodontics, Department of Medical, Oral and Biotechnological Sciences, University of Chieti, 66100 Chieti, Italy; m.vadini@unich.it (M.V.); sorrentinoed@libero.it (E.S.); virg.bif@gmail.com (V.B.); camillo.darcangelo@unich.it (C.D.)

[2] Department of Life, Health and Environmental Sciences, University of L'Aquila, 67100 L'Aquila, Italy; maurizio.damario@univaq.it (M.D.); ali-jahjah@live.fr (A.J.); massimo.frascaria@univaq.it (M.F.)

* Correspondence: fda580@gmail.com; Tel.: +39-(0)8-5454-9652

† These authors contributed equally to this work.

‡ These authors contributed equally to this work.

Abstract: To evaluate the flexural strength and flexural modulus of three recently introduced 3D-Printed resins and compare them with the flexural properties of other well known, already commercialized, and extensively used resin based dental materials. Three 3D-printed dental resins, a fiber-reinforced epoxy resin, a heat-cured bis-acrylate-based composite resin, two conventional CAD/CAM PMMA, and a graphene-reinforced CAD/CAM PMMA, were selected for this study. Ten prismatic-shaped specimens (2 × 2 × 25 mm) were fabricated for each material (n = 10). All specimens underwent a three-point bending test using a universal testing machine and were loaded until fracture. Flexural strength (MPa) and flexural modulus (MPa) mean values were calculated and compared using the on ranks One-Way ANOVA test. Scanning electron microscope analysis of the 3D-printed resins was performed. Significantly different flexural properties were recorded among the tested materials. The fiber-reinforced epoxy resin exhibited the highest flexural strength (418.0 MPa) while, among the 3D-printed resins, the best flexural strength was achieved by Irix-Max (135.0 MPa). Irix-Plus and Temporis led to the lowest mean flexural strength values (103.9 MPa and 101.3 MPa, respectively) of all the CAD/CAM milled materials, except for the conventional PMMA by Sintodent (88.9 MPa). The fiber-reinforced epoxy resin also showed the highest flexural modulus (14,672.2 MPa), followed by the heat-cured bis-acrylate composite (10,010.1 MPa). All 3D-printed resins had a higher flexural modulus than the conventional PMMA materials. CAD/CAM fiber-reinforced epoxy resin excels in flexural strength, with Irix-Max showing promising flexural properties, which could encourage its use for permanent restorations. Caution is needed with Irix-Plus and Temporis due to their lower flexural strength compared to other traditional materials.

Keywords: 3D-printed materials; CAD/CAM materials; fiber-reinforced epoxy; flexural modulus; flexural strength

Citation: De Angelis, F.; D'Amario, M.; Jahjah, A.; Frascaria, M.; Vadini, M.; Sorrentino, E.; Biferi, V.; D'Arcangelo, C. Flexural Properties of Three Novel 3D-Printed Dental Resins Compared to Other Resin-Based Restorative Materials. *Prosthesis* **2024**, *6*, 619–630. https://doi.org/10.3390/prosthesis6030043

Academic Editors: Fernando Zarone, Roberto Sorrentino and Gennaro Ruggiero

Received: 17 April 2024
Revised: 28 May 2024
Accepted: 5 June 2024
Published: 10 June 2024

1. Introduction

In restorative dentistry, resin-based materials play a crucial role. They can be employed as filling materials in both direct and indirect restorations for the treatment of tooth decay or dental defects. Direct restorations are generally indicated for small and medium cavities, while for wide cavities, indirect restorations are recommended [1].

In recent years, a possible alternative to traditional techniques for indirect restoration manufacturing has been offered by the rapid development of digital dentistry and, specifically, by Computer-Aided Design (CAD) technology. Starting from a traditional or optical impression, a digital scan of the dentition is obtained and, then, a volumetric model of the required prosthesis is produced [2]. The stereolithography (STL) file of a digital impression

can be easily transferred to the dental technician and imported into an appropriate CAD software, reducing impression taking and delivery time, patient discomfort, and vomiting reflex [3]. The specific editing tools of the software give the possibility of individualizing the restoration according to the needs of the clinician [2].

The CAD phase is followed by a Computer-Aided Manufacturing (CAM) step, which can be accomplished in different ways. The most common CAM processes are mainly subtractive, with a pre-polymerized disk/block that is reduced into the desired shape by milling. Pre-polymerized materials show superior mechanical and surface properties [4–6], improved color stability [7–9], reduced bacterial adhesion [10,11], reduced release of monomeric residue [12], and decreased clinical chairside time [13]. Other advantages of CAD/CAM systems include increased patient satisfaction [14] and, according to some findings, a fit of the intaglio surfaces [15–18] comparable to that achievable with conventional analogic methods. Nevertheless, the milling process involves a large loss of material [19], as about 90% of the prefabricated block gets wasted to make the restoration in its final shape [20].

Recently, with the introduction of 3D-printed resin materials, a new CAM solution has been made available for dental procedures. The 3D-printing industry has developed in engineering, medical, and dental fields [21,22]. The acquired STL file is transferred to a 3D printer that creates the indirect restoration following an additive (instead of a subtractive) process. Objects printed in 3D are made following layer-by-layer apposition, maintaining a high level of customization for prosthetic restoration [23]. In additive manufacturing, a serial apposition of liquid resin is placed on a support and cured by visible light, ultraviolet light, heat, or laser [24]. The process itself is relatively efficient as it does not involve tools that wear out, it limits waste production, and it allows for the simultaneous manufacturing of multiple objects [25,26], which ultimately simplifies the whole workflow [27]. According to the literature, the accuracy of 3D-printed restorations seems controversial. Based on some research, both the marginal and internal gap values seem to be lower than those obtained from milled restorations [28], but a study has shown the fit of crowns fabricated using conventional techniques and the plaster model to be better than that of a 3D-printed crown [29]. Time-consuming post-processing and high costs (for the materials and for the manufacturing devices) are some of the commonly reported disadvantages of 3D printing [30]. Moreover, the mechanical properties of 3D-printed resins may be significantly affected by printing techniques and material composition [31].

Strength is defined as the ability of a material to resist stress before plastic deforms or fractures [32]. Flexural strength is one of the most important mechanical properties for dental materials; it is proportional to tensile strength [33], and it is one of the basic parameters that are routinely considered to predict their clinical performance.

To our knowledge, few in vitro studies are available to date about the mechanical properties of 3D-printed dental materials [34–36], mainly because of their recent introduction on the market. Thus, the aim of the present research was to evaluate the flexural strength of three innovative and recently introduced 3D-printed composite resins and to compare it with the flexural strength of other already commercialized and extensively used resin-based dental materials, including a heat-cured nanohybrid bis-acrylate resin-based composite (BACR), different CAD/CAM polymethylmethacrylate (PMMA) resins, and a fiber-reinforced CAD/CAM epoxy resin. The null hypothesis to be tested was that no statistically significant differences could be detected among the different materials under investigation in terms of flexural properties.

2. Materials and Methods

The present in vitro study did not involve either human beings or human-derived tissues. For this reason, no specific IRB approval request from the local ethics committees was necessary.

A summary of the experimental groups and the material tested in the present study is given in Table 1.

Table 1. List and characteristics of the dental resins included in the experimental design.

Experimental Group	Type of Material	Manufacturing Process	Batch Number	Manufacturer	Material Trade Name
Fiber-reinforced Epoxy	CAD/CAM Fiber-reinforced Epoxy Resin	CAD/CAM milling	2208	Bioloren, Varese, Italy	Trilor
G-PMMA	CAD/CAM Graphene-reinforced Polymethyl-methacrylate	CAD/CAM milling	L18101120161	Andromeda Nanotech, Lesignano de' Bagni, Italy	G-Cam
Conventional D-PMMA	CAD/CAM Polymethyl-methacrylate	CAD/CAM milling	85196	Dentsply Sirona, Charlotte, NC, USA	Multilayer PMMA
Conventional S-PMMA	CAD/CAM Polymethyl-methacrylate	CAD/CAM milling	2247220	Sintodent, Roma, Italy	Cad-Cam shaded disc for provisional prosthesis
Irix-Max	Photosensitive ceramic filled hybrid composite	CAD/CAM 3D-printing	2314941	DWS S.r.l, Thiene, Italy	Irix Max
Irix-Plus	Photosensitive hyrid composite	CAD/CAM 3D-printing	2310941	DWS S.r.l, Thiene, Italy	Irix Plus
Temporis	Photosensitive composite	CAD/CAM 3D-printing	2301271	DWS S.r.l, Thiene, Italy	Temporis
BACR	Light and heat cured Bis-acrylate based composite resins	Conventional layering technique	2022006932	Micerium S.p.A., Avegno, Genova, Italy	Enamel Plus Biofunction

For each of the four milled CAD/CAM materials investigated (both PMMA and epoxy resin-based), ten (n = 10) prismatic specimens measuring 2 mm × 2 mm × 25 mm were shaped by milling them from a pre-polymerized disk using the conventional CAD/CAM milling method. Sample surfaces were then finalized with 180 µm grit sandpaper.

For the 3D-printed composite resins, ten (n = 10) prismatic-shaped samples were produced using a DFAB (DWS srl, Vicenza, Italy) 3D stereolithography printer and the proprietary Nauta Photoshade (DWS srl, Vicenza, Italy) software on a PC. The digital 3D model of a sample measuring 2 mm × 2 mm × 25 mm was transferred to the printer, which produced the solid three-dimensional object using a class 3B (Solid State BlueEdge) UV laser diode (DWS srl, Vicenza, Italy) to solidify the photosensitive liquid resin. A 3-minute light polymerization phase first took place in the printing machine to increase the viscosity. Once the printing process was complete, the blocks were placed in a special wash shaker containing 95% ethyl alcohol. The shaker was shaken for one minute (first wash) to remove any residual material on the surface and then blown out with compressed air. Thin supports were easily removed with the fingers thanks to the DWS "Easy Break" patent. The samples were subjected to an initial post-processing with an ultrasonic cutter. A second wash was then carried out using an airbrush with 95% ethyl alcohol and compressed air to remove any remaining material (liquid or powder). The samples were then placed in the DCURE oven, which stabilized the materials with a hybrid cycle of heat and UV light for 8 min.

In the BACR group, ten (n = 10) prismatic-shaped specimens were fabricated by pressing the uncured conventional nano-hybrid composite material in a prismatic steel mold (inner dimensions: 2 mm × 2 mm × 25 mm) between two slides with polyacetate sheets in between. The composite was then subjected to overlapping and 40 s lasting light-curing cycles on both sides with a high-power LED curing light (Celalux 3, © 2021 VOVO GmbH, Cuxhaven, Germany). After curing, the prismatic samples were removed from the mold

and finished with 180 μm grit sandpaper. The samples were then subjected to an additional 10-minute heat-curing cycle (LaborLux, Micerium) to complete the polymerization.

All prismatic specimens were loaded to failure in a universal testing machine (LR30K; Lloyd instruments Ltd., Fareham, UK) equipped with a 500 N load cell and a three-point bending test apparatus, with the span set to 20 mm. A speed of 0.5 mm/min was applied to the crossbeam of the machine. The force/deflection curve was recorded using Nexygen-Ondio software (version 4.0, Lloyd Instruments Ltd., Fareham, UK) until the mechanical failure. The load (N) and deflection (mm) were recorded.

The flexural strength (σ_f) (MPa) was calculated based on the following formula:

$$\sigma_f = 3\ F_{max}\ l/(2\ wh^2)$$

F_{max} = fracture load (N);
l = span distance (mm);
w = width of the sample (mm);
h = height of the sample (mm);

Flexural modulus (E_f) of elasticity (MPa) was calculated as the slope of the load/deflection curve in the elastic deformation range of the sample, using the following formula:

$$E_f = l^3\ F/(4\ wh^3d)$$

F = load (N);
d = deflection (mm);

Mean values and standard deviations for flexural strength and flexural modulus were calculated for each test group. The Shapiro-Wilk test and Brown-Forsythe test did not, respectively, confirm the normality and homoscedasticity of the data set ($p < 0.05$). Therefore, median values were compared using Kruskal-Wallis One-Way Analysis of Variance on Ranks. All pairwise multiple comparisons were performed using the Student–Newman–Keuls method.

Scanning Electron Microscope (SEM) Analysis

Representative specimens from each one of the three 3D-printed resin groups (Irix-Max, Irix-Plus, and Temporis) were gold sputtered (Emitech K550; Emitech Ltd., Ashford, Kent, UK), and scanning electron microscope (SEM) images were taken at 100×, 1000× and 3000× magnifications, in order to observe any possible trace of the additive layering on the specimen surface and to qualitatively evaluate the presence of filler particles. SEM analysis was carried out using an EVO 50 XVP LaB6 (Carl Zeiss SMT Ltd., Cambridge, UK) operating at 15 kV and in high-vacuum mode.

3. Results

The mean values (and the standard deviations) for the flexural strength (MPa) and the flexural modulus (MPa) achieved in the eight experimental groups tested are summarized in Table 2.

A significantly increased Flexural Strength was detected in the fiber-reinforced Epoxy group, as compared to all the other materials tested.

In terms of flexural strength, statistically significant differences were detected among almost all the experimental groups tested, except for the Irix-Plus VS Temporis group comparison. In particular, concerning 3D-printed resins, Flexural Strength (MPa) and Flexural Modulus (MPa) values, respectively, achieved in Irix-Plus (103.9 MPa/2750.8 MPa) and Temporis (101.3 MPa/2824.2 MPa) groups were not statistically different, but a significant difference emerged comparing them to the Irix-Max (135.0 MPa/4429.1 MPa).

Table 2. Mean values and standard deviations for flexural strength (MPa) and flexural modulus (MPa).

Experimental Group	Flexural Strength (MPa)	Flexural Modulus (MPa)
Fiber-reinforced Epoxy	418.0 [a] (51.0)	14,672.2 [a] (1296.5)
Irix-Max	135.0 [b] (2.3)	4429.1 [c] (570.6)
BACR	127.9 [c] (17.6)	10,010.1 [b] (720.6)
G-PMMA	120.1 [d] (9.7)	2700.2 [d] (180.8)
Conventional D-PMMA	113.3 [e] (13.7)	2506.8 [e] (485.4)
Irix-Plus	103.9 [f] (3.8)	2750.2 [d] (260.9)
Temporis	101.3 [f] (6.4)	2824.2 [d] (219.7)
Conventional S-PMMA	88.9 [g] (6.7)	2137.2 [f] (149.6)

Different superscript letters indicate statistically significant differences.

The highest flexural modulus was recorded in the fiber-reinforced epoxy group, which significantly increased compared to all the other materials. The BACR group showed a flexural modulus value of 10,010.1 MPa, significantly higher than that of all the PMMA-based and 3D-printed materials.

Flexural strength tests of the three 3D-printed resins (Irix-Max, Irix-Plus, and Temporis) are shown in Video S1 as Supplementary Materials.

The SEM analysis of the 3D-printed resins, with images taken at 100× magnifications, clearly highlighted the presence of a horizontal pattern perpendicular to the printing orientation (Figure 1). SEM images taken at higher magnifications (1000× and 3000×) showed the presence of spheric inclusions (approximately ranging between 1 and 8µm in diameter), corresponding to the filler particles embedded within the resin matrix (Figure 2). The number of particles appeared to be higher in Irix-Max than in Irix-Plus. Temporis showed the least number of filler particles.

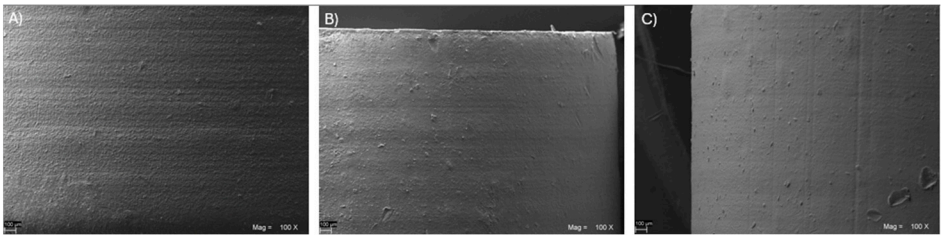

Figure 1. SEM images (original magnification 100×) of Irix-Max (**A**), Irix-Plus (**B**) and Temporis (**C**) showing signs of horizontal pattern due to the printing process.

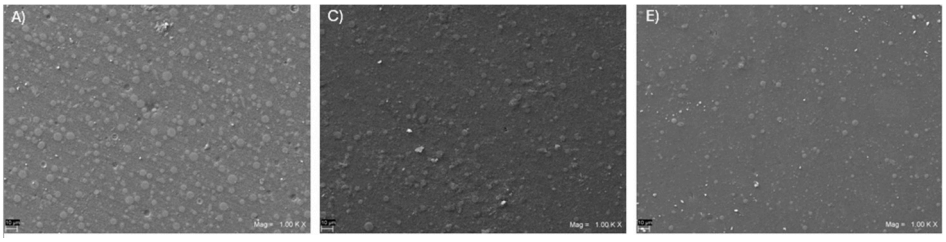

Figure 2. *Cont.*

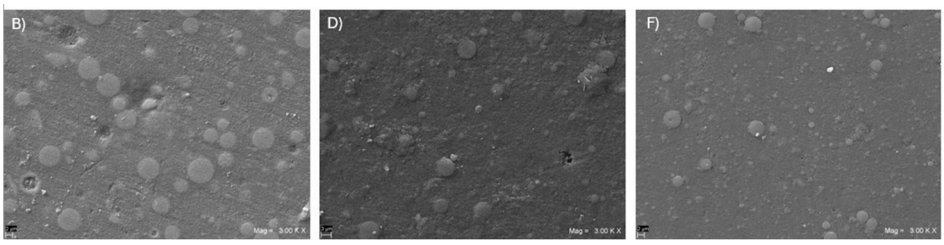

Figure 2. SEM images of Irix-Max (**A**,**B**), Irix-Plus (**C**,**D**) and Temporis (**E**,**F**) showing the presence of filler particles embedded within the resin matrix. Original magnifications, 1000× (**A**,**C**,**E**) and 3000× (**B**,**D**,**F**).

4. Discussion

The purpose of the present study was to compare the flexural strength and flexural modulus of three innovative 3D-printed dental resins with the flexural properties of other CAD/CAM-milled dental materials already on the market (a graphene-reinforced PMMA, two different conventional PMMAs, a fiber-reinforced epoxy resin), and a conventional layered and heat-cured bis-acrylate-based nanohybrid composite. Such a purpose seems to be of paramount importance, especially considering that few studies on the flexural properties of 3D-printed dental resins are currently available in the literature [34–36], and flexural strength data should be carefully considered when selecting innovative resins as permanent restorative materials.

The null hypothesis tested in the present study had to be rejected. In fact, significant differences in flexural properties could be detected among the tested materials. The values of flexural strength and flexural modulus are considered indicators of the ultimate material mechanical resistance in normal clinical situations. The three-point bending test in particular is widely regarded as the most valid flexural strength test compared to other test arrangements due to its lower standard deviation, lower coefficient of variation, and lower crack distribution [37].

According to some manufacturers, a high flexural modulus should be seen as a significant benefit for dental materials [30]. However, this is not always consistent with the mechanical properties of many dental resins currently available on the market. For instance, Flexcera™ Dental 3D-printed resin (Desktop Health™, Dearborn, MI, USA) and Graphy—Tera Hartz TC-85 DAC (Yen co., Treviso, Italy) have specifically been created to have a lower flexural modulus. As previously postulated by Magne et al. [38], materials with a lower flexural modulus experience a bigger deformation under load and greater stress absorption than those characterized by a higher flexural modulus.

Based on literature data, CAD/CAM materials seem to show a relatively high flexural strength and a low flexural modulus [39,40], probably due to an increased filler load and enhanced degree of cure [41]. In the present paper, fiber-reinforced epoxy resin showed the highest flexural strength values. Also in previous studies, fiber-reinforced epoxy resins showed better fracture resistance than conventional resin-based dental materials [42,43]. Their improved mechanical properties can be mainly related to the fibers limiting crack initiation and propagation [43]. Fiber type, orientation, distribution, aspect ratio, volume fraction, and crosslinking at the fiber–resin interface can play a key role in the ultimate material reinforcement [44].

In our study, the 3D-printed Irix-Max showed a slightly increased flexural strength if compared to the heat-cured BACR. Irix-Plus and Temporis showed lower flexural strength than G-PMMA and Conventional D-PMMA resins, but higher values than Conventional S-PMMA. Irix-Max seemed to guarantee the best flexural strength among the three 3D-printed materials tested.

The flexural properties of 3D-printed resins could be affected by the printing technique [45] and, in particular, by "pre-printing", "printing", and "post-printing" factors [46]. The study by Borella et al. [47] precisely detailed how various 3D printing configurations may influence the characteristics of dental artifacts. The analysis demonstrates that critical

factors such as post-curing, nesting, and layer orientation directly impact the quality of the finished products. Artifacts with optimized post-curing achieved an average deviation from trueness of only 0.05 mm, indicating excellent dimensional accuracy compared to the original models. In contrast, sub-optimal nesting settings increased residual stresses, with average deviations ranging from 0.1 mm to 0.2 mm, suggesting reduced dimensional precision. The study also explored the variation in layer orientation, finding that an optimal angle of 45° relative to the printing platform resulted in improved trueness, with less visible layer lines and minimal distortion.

In detail about "pre-printing" factors, several studies reported that the addition of appropriate fillers could enhance the mechanical properties of 3D-printed resins [34,48,49]. Of course, added fillers should not negatively affect the resin color, fluidity, or light penetration [46].

Concerning "printing" factors, the flexural strength of 3D-printed resins is also inversely proportional to the printed layer thickness [35], and it seems to be affected by the printing orientation. Some authors observed a higher flexural strength with a 0° printing orientation [26,50,51]; however, Väyrynen et al. [52] reported a better flexural strength with a 45° printing orientation, and two studies observed better flexural properties with a 90° printing orientation [52,53]. Specimens realized with a 0° orientation were found to be affected by layer adhesion [26], whereas vertically printed samples are affected by resin type, adhesion surface dimension, and polymerization rates [26].

As far as "post-printing" factors are concerned, a significant impact of the curing unit on the flexural strength of 3D-printed resins has been demonstrated [35,54,55]. Moreover, the photo-initiator may affect their color and their mechanical properties [56,57], as the activation of the photo-initiator at the proper wavelength promotes greater polymer conversion [55]. Thus, an appropriate time exposure to the curing source and an adequate combination of photo-initiator and co-initiator may significantly affect the mechanical strength of 3D-printed resins [58].

In our study, all printed samples were prepared using consistent parameters. Moreover, the printing parameters cannot be modified by the operator and remain constant. However, maybe due to the numerous "pre-printing", "printing" and "post-printing" factors able to influence the material quality, the literature data so far available about 3D-printed resin are still controversial.

Some authors observed superior flexural strength results for 3D-printed resins than for CAD/CAM-milled PMMA [59]. According to a study by Valenti et al. [60], 3D-printed materials are a good alternative to conventionally milled ones. Concerning CAD/CAM PMMA-milled materials, monomer release after aging [61], the effects of milling [36,62], and a high carbon/oxygen weight percentage [63] may be some of the reasons for their reduced mechanical properties in comparison to 3D-printed resins. With regard to the subtractive techniques for the realization of samples made by CAD/CAM milling technology, the fabrication process and the use of diamond burs could lead to material weakness, increasing the risk of fracture [64]. These defects should hypothetically lead to reduced fracture resistance compared to that of 3D-printed additive materials.

In contrast to the abovementioned data, similar mechanical properties were recorded by Taşın et al. between CAD/CAM-milled PMMA and 3D-printed resins [65]. While other authors reported an even lower fracture resistance for 3D-printed prosthetic materials. Digholkar et al. [66], for instance, recorded superior flexural strength for CAD/CAM milled PMMA. As a result of such inconsistent findings, prostheses fabricated by 3D-printed materials are still mainly used for temporary restorations.

The relevance and originality of the present research mainly lie in the relatively recent introduction of 3D-printed materials for dental purposes and the subsequent limited availability of independent studies investigating their mechanical properties. In such scenarios, collecting new data allows a useful comparison with the few data to date available. According to a study conducted by Pantea et al. [67], 3D-printed resins from HARTZ Labs Dental Sands and 3D-printed from NextDent C&B MFH (141 MPa and

143 MPa, respectively) demonstrated a similar flexural strength compared to the Irix Max (135 MPa) after the bending test. In another study by Taşin et al. [65], the mechanical properties of 3D-printed Temporis were tested using a 3-point bending test. The study reported a flexural modulus of 3357 MPa (standard deviation 282 MPa), whereas in the present study, the same material showed a flexural modulus of 2842 MPa. Additionally, the flexural strength was 85 MPa (standard deviation 1 MPa) in their study, compared to 101 MPa in the present study. A study by Revilla-León et al. [68] analyzed the mechanical properties of Temporis and compared the results to those of other materials. Specifically, they tested the flexural strength and flexural modulus (85–135 Mpa and 2900–4200 MPa, respectively) and obtained results very similar to those herein observed (101.3 MPa and 2824.2 MPa, respectively).

As for the clinical significance of the present research, comparing the flexural strength of the new 3D-printed resins with that of other well established permanent restorative materials may represent a valid in vitro method able to suggest if the new materials might show acceptable intraoral performances and reliability. Based on the mechanical differences detected among the materials evaluated in this study, the present outcomes suggest that, concerning 3D-printed resins, Irix-Max could be safely used as a permanent restorative material, while for Irix-Plus and Temporis further investigation seems required. It should be underlined that in technical data sheets, the detailed composition of Irix-Max, Irix-Plus, and Temporis composites cannot be retrieved. However, as already suggested in previous studies [34,48,49], a favorable combination of fillers within the 3D-resin formulations could be a reasonable explanation for the promising mechanical properties herein observed, mainly concerning Irix-Max.

Regarding fiber-reinforced materials, the optimal flexural strength recorded in the present study confirm them as an ideal choice for relatively lightweight but still resistant and reliable prosthetic substructures.

In the present study, a graphene-reinforced PMMA was also investigated; its flexural strength was slightly superior to the other conventional PMMAs tested but lower than Irix-Max and the heat-cured BACR. Experimental attempts were recently made to create a uniform dispersion of graphene nanofillers in the polymer matrix through a change in graphene surface chemistry and its interaction with the polymer matrix [69,70]. This was usually achieved through hydrogen bonding or covalent functionalization. Unprecedently, Wand G. et al. showed that the impact of surface functionalization and degrees of graphene on the interfacial adhesion of G-PMMA explains the value of optimized chemical functionalization on the interfacial stress transfer and fracture mechanism at a microscopic level. In addition, the presence of the oxidative debris in the graphene oxide could help the formation of G-PMMA, which is due to a good dispersion and strong interfacial interaction between graphene and polymer matrix [71]. According to other studies, an optimized fusion of graphene in PMMA materials might further strengthen the resin's mechanical properties [72]. The exact amount of graphene added to the G-PMMA tested in this study is not disclosed by the manufacturer. A hypothetically too low concentration of graphene [73] could be a reasonable explanation for the still "improvable" flexural properties herein observed.

The present paper evaluated the flexural strength and flexural modulus of three recently introduced 3D-printed resin-based dental materials, comparing them to various CAD/CAM milled resins and a heat-cured bis-acrylate resin composite, with all the advantages and limitations of an in vitro study design. Indeed, the properties of resin materials observed in clinical settings may differ from those detected in laboratories. This study only reported the flexural strength and flexural modulus. Thus, as a purpose for further research, additional tests such as Vickers microhardness, wear resistance, and compressive strength might be performed to better understand the overall mechanical behaviors of the tested materials.

5. Conclusions

Based on the findings of the present in vitro study, the following conclusions can be drawn:

(1) CAD/CAM fiber-reinforced epoxy resins seem to show superior flexural strength and the highest flexural modulus of elasticity amongst the resin-based dental materials;
(2) Different 3D-printed resins may show significant differences in flexural properties when compared to one another;
(3) In terms of flexural strength, Irix-Max seems the more promising among the different 3D-printed resins, with a flexural strength that may be even superior to conventional heat-cured BACRs, justifying its safe use as a permanent restorative material;
(4) The other two 3D-printed resins tested, Irix-Plus and Temporis, showed superior flexural strength compared to the conventional S-PMMA (by Sintodent) but reduced performances when compared to G-PMMA and the conventional D-PMMA (by Dentsply-Sirona), so their use as permanent restorative materials should be still considered with some caution.

Supplementary Materials: The following supporting information can be downloaded at: https://www.mdpi.com/article/10.3390/prosthesis6030043/s1, Video S1: Video 1—3d-printed resin flexural strength test.

Author Contributions: Conceptualization, F.D.A., M.D., M.V. and C.D.; software, F.D.A., E.S. and V.B.; methodology, F.D.A., M.D., M.V., E.S., V.B. and C.D.; formal analysis, F.D.A.; investigation, M.D., A.J., M.V., E.S. and V.B.; resources, F.D.A., M.D., M.V., M.F. and C.D.; data curation, F.D.A.; writing—original draft preparation, A.J., E.S. and V.B.; writing—review and editing, F.D.A., M.D., E.S. and V.B.; supervision, F.D.A., M.D., M.V., M.F. and C.D.; project administration, C.D.; funding acquisition, F.D.A. and C.D.; All authors have read and agreed to the published version of the manuscript.

Funding: This research received no external funding.

Data Availability Statement: The data presented in this study are available on request from the corresponding author.

Conflicts of Interest: The authors declare no conflicts of interests.

References

1. Ferracane, J.L. Resin composite—State of the art. *Dent. Mater.* **2011**, *27*, 29–38. [CrossRef]
2. Fasbinder, D.J. Computerized technology for restorative dentistry. *Am. J. Dent.* **2013**, *26*, 115–120.
3. Takeuchi, Y.; Koizumi, H.; Furuchi, M.; Sato, Y.; Ohkubo, C.; Matsumura, H. Use of digital impression systems with intraoral scanners for fabricating restorations and fixed dental prostheses. *J. Oral Sci.* **2018**, *60*, 1–7. [CrossRef] [PubMed]
4. Aguirre, B.C.; Chen, J.H.; Kontogiorgos, E.D.; Murchison, D.F.; Nagy, W.W. Flexural strength of denture base acrylic resins processed by conventional and cad-cam methods. *J. Prosthet. Dent.* **2020**, *123*, 641–646. [CrossRef]
5. Al-Dwairi, Z.N.; Tahboub, K.Y.; Baba, N.Z.; Goodacre, C.J. A comparison of the flexural and impact strengths and flexural modulus of cad/cam and conventional heat-cured polymethyl methacrylate (pmma). *J. Prosthodont.* **2020**, *29*, 341–349. [CrossRef] [PubMed]
6. Al-Dwairi, Z.N.; Tahboub, K.Y.; Baba, N.Z.; Goodacre, C.J.; Özcan, M. A comparison of the surface properties of cad/cam and conventional polymethylmethacrylate (pmma). *J. Prosthodont.* **2019**, *28*, 452–457. [CrossRef] [PubMed]
7. Al-Qarni, F.D.; Goodacre, C.J.; Kattadiyil, M.T.; Baba, N.Z.; Paravina, R.D. Stainability of acrylic resin materials used in cad-cam and conventional complete dentures. *J. Prosthet. Dent.* **2020**, *123*, 880–887. [CrossRef]
8. Gruber, S.; Kamnoedboon, P.; Özcan, M.; Srinivasan, M. Cad/cam complete denture resins: An in vitro evaluation of color stability. *J. Prosthodont.* **2021**, *30*, 430–439. [CrossRef]
9. Alp, G.; Johnston, W.M.; Yilmaz, B. Optical properties and surface roughness of prepolymerized poly(methyl methacrylate) denture base materials. *J. Prosthet. Dent.* **2019**, *121*, 347–352. [CrossRef]
10. Murat, S.; Alp, G.; Alatalı, C.; Uzun, M. In vitro evaluation of adhesion of candida albicans on cad/cam pmma-based polymers. *J. Prosthodont.* **2019**, *28*, e873–e879. [CrossRef]
11. Al-Fouzan, A.F.; Al-Mejrad, L.A.; Albarrag, A.M. Adherence of candida to complete denture surfaces in vitro: A comparison of conventional and cad/cam complete dentures. *J. Adv. Prosthodont.* **2017**, *9*, 402–408. [CrossRef] [PubMed]
12. Ayman, A.D. The residual monomer content and mechanical properties of cad\cam resins used in the fabrication of complete dentures as compared to heat cured resins. *Electron. Physician* **2017**, *9*, 4766–4772. [CrossRef] [PubMed]

13. Srinivasan, M.; Schimmel, M.; Naharro, M.; O'Neill, C.; McKenna, G.; Müller, F. Cad/cam milled removable complete dentures: Time and cost estimation study. *J. Dent.* **2019**, *80*, 75–79. [CrossRef] [PubMed]
14. Kattadiyil, M.T.; Jekki, R.; Goodacre, C.J.; Baba, N.Z. Comparison of treatment outcomes in digital and conventional complete removable dental prosthesis fabrications in a predoctoral setting. *J. Prosthet. Dent.* **2015**, *114*, 818–825. [CrossRef] [PubMed]
15. Hsu, C.Y.; Yang, T.C.; Wang, T.M.; Lin, L.D. Effects of fabrication techniques on denture base adaptation: An in vitro study. *J. Prosthet. Dent.* **2020**, *124*, 740–747. [CrossRef] [PubMed]
16. McLaughlin, J.B.; Ramos, V., Jr.; Dickinson, D.P. Comparison of fit of dentures fabricated by traditional techniques versus cad/cam technology. *J. Prosthodont.* **2019**, *28*, 428–435. [CrossRef] [PubMed]
17. Srinivasan, M.; Cantin, Y.; Mehl, A.; Gjengedal, H.; Müller, F.; Schimmel, M. Cad/cam milled removable complete dentures: An in vitro evaluation of trueness. *Clin. Oral Investig.* **2017**, *21*, 2007–2019. [CrossRef] [PubMed]
18. Goodacre, B.J.; Goodacre, C.J.; Baba, N.Z.; Kattadiyil, M.T. Comparison of denture base adaptation between cad-cam and conventional fabrication techniques. *J. Prosthet. Dent.* **2016**, *116*, 249–256. [CrossRef] [PubMed]
19. Kalberer, N.; Mehl, A.; Schimmel, M.; Müller, F.; Srinivasan, M. Cad-cam milled versus rapidly prototyped (3d-printed) complete dentures: An in vitro evaluation of trueness. *J. Prosthet. Dent.* **2019**, *121*, 637–643. [CrossRef]
20. Wang, W.; Yu, H.; Liu, Y.; Jiang, X.; Gao, B. Trueness analysis of zirconia crowns fabricated with 3-dimensional printing. *J. Prosthet. Dent.* **2019**, *121*, 285–291. [CrossRef]
21. Shubert, J.; Bell, M.A.L. Photoacoustic imaging of a human vertebra: Implications for guiding spinal fusion surgeries. *Phys. Med. Biol.* **2018**, *63*, 144001. [CrossRef]
22. Best, C.; Strouse, R.; Hor, K.; Pepper, V.; Tipton, A.; Kelly, J.; Shinoka, T.; Breuer, C. Toward a patient-specific tissue engineered vascular graft. *J. Tissue Eng.* **2018**, *9*, 2041731418764709. [CrossRef] [PubMed]
23. Barazanchi, A.; Li, K.C.; Al-Amleh, B.; Lyons, K.; Waddell, J.N. Additive technology: Update on current materials and applications in dentistry. *J. Prosthodont.* **2017**, *26*, 156–163. [CrossRef] [PubMed]
24. Revilla-León, M.; Özcan, M. Additive manufacturing technologies used for processing polymers: Current status and potential application in prosthetic dentistry. *J. Prosthodont.* **2019**, *28*, 146–158. [CrossRef] [PubMed]
25. Kattadiyil, M.T.; AlHelal, A. An update on computer-engineered complete dentures: A systematic review on clinical outcomes. *J. Prosthet. Dent.* **2017**, *117*, 478–485. [CrossRef] [PubMed]
26. Shim, J.S.; Kim, J.E.; Jeong, S.H.; Choi, Y.J.; Ryu, J.J. Printing accuracy, mechanical properties, surface characteristics, and microbial adhesion of 3d-printed resins with various printing orientations. *J. Prosthet. Dent.* **2020**, *124*, 468–475. [CrossRef] [PubMed]
27. Lin, L.; Fang, Y.; Liao, Y.; Chen, G.; Gao, C.; Zhu, P. 3d printing and digital processing techniques in dentistry: A review of literature. *Adv. Healthc. Mater.* **2019**, *21*, 1801013. [CrossRef]
28. Alharbi, N.; Alharbi, S.; Cuijpers, V.; Osman, R.B.; Wismeijer, D. Three-dimensional evaluation of marginal and internal fit of 3d-printed interim restorations fabricated on different finish line designs. *J. Prosthodont. Res.* **2018**, *62*, 218–226. [CrossRef] [PubMed]
29. Jang, Y.; Sim, J.Y.; Park, J.K.; Kim, W.C.; Kim, H.Y.; Kim, J.H. Evaluation of the marginal and internal fit of a single crown fabricated based on a three-dimensional printed model. *J. Adv. Prosthodont.* **2018**, *10*, 367–373. [CrossRef]
30. Tian, Y.; Chen, C.; Xu, X.; Wang, J.; Hou, X.; Li, K.; Lu, X.; Shi, H.; Lee, E.S.; Jiang, H.B. A review of 3d printing in dentistry: Technologies, affecting factors, and applications. *Scanning* **2021**, *2021*, 9950131. [CrossRef]
31. Atria, P.J.; Bordin, D.; Marti, F.; Nayak, V.V.; Conejo, J.; Jalkh, E.B.; Witek, L.; Sampaio, C.S. 3d-printed resins for provisional dental restorations: Comparison of mechanical and biological properties. *J. Esthet. Restor. Dent.* **2022**, *34*, 804–815. [CrossRef] [PubMed]
32. Mecholsky, J.J., Jr. Fracture mechanics principles. *Dent. Mater.* **1995**, *11*, 111–112. [CrossRef] [PubMed]
33. Kim, J.H.; Ko, K.H.; Huh, Y.H.; Park, C.J.; Cho, L.R. Effects of the thickness ratio of zirconia-lithium disilicate bilayered ceramics on the translucency and flexural strength. *J. Prosthodont.* **2020**, *29*, 334–340. [CrossRef]
34. Aati, S.; Akram, Z.; Ngo, H.; Fawzy, A.S. Development of 3d printed resin reinforced with modified zro(2) nanoparticles for long-term provisional dental restorations. *Dent. Mater.* **2021**, *37*, e360–e374. [CrossRef]
35. Perea-Lowery, L.; Gibreel, M.; Vallittu, P.K.; Lassila, L. Evaluation of the mechanical properties and degree of conversion of 3d printed splint material. *J. Mech. Behav. Biomed. Mater.* **2021**, *115*, 104254. [CrossRef]
36. Tahayeri, A.; Morgan, M.; Fugolin, A.P.; Bompolaki, D.; Athirasala, A.; Pfeifer, C.S.; Ferracane, J.L.; Bertassoni, L.E. 3d printed versus conventionally cured provisional crown and bridge dental materials. *Dent. Mater.* **2018**, *34*, 192–200. [CrossRef]
37. Chung, S.M.; Yap, A.U.; Chandra, S.P.; Lim, C.T. Flexural strength of dental composite restoratives: Comparison of biaxial and three-point bending test. *J. Biomed. Mater. Res. B Appl. Biomater.* **2004**, *71*, 278–283. [CrossRef] [PubMed]
38. Magne, P.; Paranhos, M.P.G.; Burnett, L.H., Jr.; Magne, M.; Belser, U.C. Fatigue resistance and failure mode of novel-design anterior single-tooth implant restorations: Influence of material selection for type iii veneers bonded to zirconia abutments. *Clin. Oral. Implant. Res.* **2011**, *22*, 195–200. [CrossRef]
39. Alharbi, N.; Osman, R.; Wismeijer, D. Effects of build direction on the mechanical properties of 3d-printed complete coverage interim dental restorations. *J. Prosthet. Dent.* **2016**, *115*, 760–767. [CrossRef]
40. Sulaiman, T.A. Materials in digital dentistry-a review. *J. Esthet. Restor. Dent.* **2020**, *32*, 171–181. [CrossRef]
41. Zimmermann, M.; Ender, A.; Attin, T.; Mehl, A. Fracture load of three-unit full-contour fixed dental prostheses fabricated with subtractive and additive cad/cam technology. *Clin. Oral. Investig.* **2020**, *24*, 1035–1042. [CrossRef] [PubMed]

42. Patnana, A.K.; Vanga, N.R.V.; Vabbalareddy, R.; Chandrabhatla, S.K. Evaluating the fracture resistance of fiber reinforced composite restorations—An in vitro analysis. *Indian. J. Dent. Res.* **2020**, *31*, 138–144. [CrossRef] [PubMed]
43. Tsujimoto, A.; Barkmeier, W.W.; Takamizawa, T.; Latta, M.A.; Miyazaki, M. Mechanical properties, volumetric shrinkage and depth of cure of short fiber-reinforced resin composite. *Dent. Mater. J.* **2016**, *35*, 418–424. [CrossRef] [PubMed]
44. Lassila, L.; Keulemans, F.; Vallittu, P.K.; Garoushi, S. Characterization of restorative short-fiber reinforced dental composites. *Dent. Mater. J.* **2020**, *39*, 992–999. [CrossRef] [PubMed]
45. Gad, M.M.; Fouda, S.M.; Abualsaud, R.; Alshahrani, F.A.; Al-Thobity, A.M.; Khan, S.Q.; Akhtar, S.; Ateeq, I.S.; Helal, M.A.; Al-Harbi, F.A. Strength and surface properties of a 3d-printed denture base polymer. *J. Prosthodont.* **2022**, *31*, 412–418. [CrossRef] [PubMed]
46. Gad, M.M.; Fouda, S.M. Factors affecting flexural strength of 3d-printed resins: A systematic review. *J. Prosthodont.* **2023**, *32*, 96–110. [CrossRef] [PubMed]
47. Borella, P.S.; Alvares, L.A.; Ribeiro, M.T.; Moura, G.F.; Soares, C.J.; Zancopé, K.; Mendonça, G.; Rodrigues, F.P.; das Neves, F.D. Physical and mechanical properties of four 3d-printed resins at two different thick layers: An in vitro comparative study. *Dent. Mater.* **2023**, *39*, 686–692. [CrossRef]
48. Chen, S.; Yang, J.; Jia, Y.G.; Lu, B.; Ren, L. A study of 3d-printable reinforced composite resin: Pmma modified with silver nanoparticles loaded cellulose nanocrystal. *Materials* **2018**, *11*, 2444. [CrossRef]
49. Gad, M.M.; Al-Harbi, F.A.; Akhtar, S.; Fouda, S.M. 3d-printable denture base resin containing sio(2) nanoparticles: An in vitro analysis of mechanical and surface properties. *J. Prosthodont.* **2022**, *31*, 784–790. [CrossRef]
50. Derban, P.; Negrea, R.; Rominu, M.; Marsavina, L. Influence of the printing angle and load direction on flexure strength in 3d printed materials for provisional dental restorations. *Materials* **2021**, *14*, 3376. [CrossRef]
51. Srinivasan, M.; Kalberer, N.; Kamnoedboon, P.; Mekki, M.; Durual, S.; Özcan, M.; Müller, F. Cad-cam complete denture resins: An evaluation of biocompatibility, mechanical properties, and surface characteristics. *J. Dent.* **2021**, *114*, 103785. [CrossRef] [PubMed]
52. Väyrynen, V.O.; Tanner, J.; Vallittu, P.K. The anisotropicity of the flexural properties of an occlusal device material processed by stereolithography. *J. Prosthet. Dent.* **2016**, *116*, 811–817. [CrossRef] [PubMed]
53. Unkovskiy, A.; Bui, P.H.-B.; Schille, C.; Geis-Gerstorfer, J.; Huettig, F.; Spintzyk, S. Objects build orientation, positioning, and curing influence dimensional accuracy and flexural properties of stereolithographically printed resin. *Dent. Mater.* **2018**, *34*, e324–e333. [CrossRef] [PubMed]
54. Perea-Lowery, L.; Gibreel, M.; Vallittu, P.K.; Lassila, L.V. 3d-printed vs. Heat-polymerizing and autopolymerizing denture base acrylic resins. *Materials* **2021**, *14*, 5781. [CrossRef] [PubMed]
55. Li, P.; Lambart, A.L.; Stawarczyk, B.; Reymus, M.; Spintzyk, S. Postpolymerization of a 3d-printed denture base polymer: Impact of post-curing methods on surface characteristics, flexural strength, and cytotoxicity. *J. Dent.* **2021**, *115*, 103856. [CrossRef]
56. Shin, D.-H.; Rawls, H.R. Degree of conversion and color stability of the light curing resin with new photoinitiator systems. *Dent. Mater.* **2009**, *25*, 1030–1038. [CrossRef] [PubMed]
57. Albuquerque, P.P.A.; Moreira, A.D.; Moraes, R.R.; Cavalcante, L.M.; Schneider, L.F.J. Color stability, conversion, water sorption and solubility of dental composites formulated with different photoinitiator systems. *J. Dent.* **2013**, *41*, e67–e72. [CrossRef] [PubMed]
58. Bayarsaikhan, E.; Lim, J.H.; Shin, S.H.; Park, K.H.; Park, Y.B.; Lee, J.H.; Kim, J.E. Effects of postcuring temperature on the mechanical properties and biocompatibility of three-dimensional printed dental resin material. *Polymers* **2021**, *13*, 1180. [CrossRef] [PubMed]
59. Park, S.M.; Park, J.M.; Kim, S.K.; Heo, S.J.; Koak, J.Y. Flexural strength of 3d-printing resin materials for provisional fixed dental prostheses. *Materials* **2020**, *13*, 3970. [CrossRef]
60. Valenti, C.; Federici, M.I.; Masciotti, F.; Marinucci, L.; Xhimitiku, I.; Cianetti, S.; Pagano, S. Mechanical properties of 3d-printed prosthetic materials compared with milled and conventional processing: A systematic review and meta-analysis of in vitro studies. *J. Prosthet. Dent.* **2022**. [CrossRef]
61. Duarte, S.; Sartori, N.; Phark, J.-H. Ceramic-reinforced polymers: Cad/cam hybrid restorative materials. *Curr. Oral Health Rep.* **2016**, *3*, 198–202. [CrossRef]
62. Curran, P.; Cattani-Lorente, M.; Wiskott, H.W.A.; Durual, S.; Scherrer, S.S. Grinding damage assessment for cad-cam restorative materials. *Dent. Mater.* **2017**, *33*, 294–308. [CrossRef] [PubMed]
63. Ibrahim, A.; El Shehawy, D.; El-Naggar, G.J.A.S.D.J. Fracture resistance of interim restoration constructed by 3d printing versus cad/cam technique (in vitro study). *Egypt. Dent. J.* **2020**, *23*, 13–20.
64. Corbani, K.; Hardan, L.; Skienhe, H.; Özcan, M.; Alharbi, N.; Salameh, Z. Effect of material thickness on the fracture resistance and failure pattern of 3d-printed composite crowns. *Int. J. Comput. Dent.* **2020**, *23*, 225–233. [PubMed]
65. Taşın, S.; Ismatullaev, A. Comparative evaluation of the effect of thermocycling on the mechanical properties of conventionally polymerized, cad-cam milled, and 3d-printed interim materials. *J. Prosthet. Dent.* **2022**, *127*, 173.e1–173.e8. [CrossRef] [PubMed]
66. Digholkar, S.; Madhav, V.N.; Palaskar, J. Evaluation of the flexural strength and microhardness of provisional crown and bridge materials fabricated by different methods. *J. Indian. Prosthodont. Soc.* **2016**, *16*, 328–334. [CrossRef] [PubMed]
67. Pantea, M.; Ciocoiu, R.C.; Greabu, M.; Totan, A.R.; Imre, M.; Țâncu, A.M.C.; Sfeatcu, R.; Spînu, T.C.; Ilinca, R.; Petre, A.E. Compressive and flexural strength of 3d-printed and conventional resins designated for interim fixed dental prostheses: An in vitro comparison. *Materials* **2022**, *15*, 3075. [CrossRef] [PubMed]

68. Revilla-León, M.; Meyers, M.J.; Zandinejad, A.; Özcan, M. A review on chemical composition, mechanical properties, and manufacturing work flow of additively manufactured current polymers for interim dental restorations. *J. Esthet. Restor. Dent.* **2019**, *31*, 51–57. [CrossRef] [PubMed]
69. Wang, G.; Dai, Z.; Liu, L.; Hu, H.; Dai, Q.; Zhang, Z. Tuning the interfacial mechanical behaviors of monolayer graphene/pmma nanocomposites. *ACS Appl. Mater. Interfaces* **2016**, *8*, 22554–22562. [CrossRef]
70. Hu, X.; Su, E.; Zhu, B.; Jia, J.; Yao, P.; Bai, Y. Preparation of silanized graphene/poly (methyl methacrylate) nanocomposites in situ copolymerization and its mechanical properties. *Compos. Sci. Technol.* **2014**, *97*, 6–11. [CrossRef]
71. Vallés, C.; Kinloch, I.A.; Young, R.J.; Wilson, N.R.; Rourke, J.P. Graphene oxide and base-washed graphene oxide as reinforcements in pmma nanocomposites. *Compos. Sci. Technol.* **2013**, *88*, 158–164. [CrossRef]
72. Bacali, C.; Badea, M.; Moldovan, M.; Sarosi, C.; Nastase, V.; Baldea, I.; Chiorean, R.S.; Constantiniuc, M. The influence of graphene in improvement of physico-mechanical properties in pmma denture base resins. *Materials* **2019**, *12*, 2335. [CrossRef] [PubMed]
73. De Angelis, F.; Vadini, M.; Buonvivere, M.; Valerio, A.; Di Cosola, M.; Piattelli, A.; Biferi, V.; D'Arcangelo, C. In vitro mechanical properties of a novel graphene-reinforced pmma-based dental restorative material. *Polymers* **2023**, *15*, 622. [CrossRef] [PubMed]